DRAMATIC BOND STRENGTH ALTERATIONS INDUCED ON A "ROUGH" SURFACE BY SMALL SUPERFICIAL METALLIC ISLANDS. I. EFFECT OF ISLAND SIZE AND SHAPE

Christian MINOT [1], John P. LOWE [2] and Lionel SALEM [3]

Laboratoire de Chimie Théorique, URA 506, Université de Paris-Sud, 91405 Orsay, France

Received 12 October 1989; accepted 12 December 1989

Hückel method, surface restructuring, heterogeneous catalysis, metallic surfaces

Islands of different size and shape (square or linear, finite or infinite) are introduced at the FCC positions above a single (100) layer of atoms (one s orbital per atom) in order to represent the roughness of the surface. The extended Hückel method with periodic boundary conditions shows the overlap population *between the surface atoms* near the islands to be strongly modified. Certain bonds are dramatically weakened, others dramatically strengthened. As immediate consequences the surface is prepared for subsequent restructuring and is activated for heterogeneous catalysis. Depending on the nature of the island (*island* specificity) and on the band occupancy (*metal* specificity), a given bond may be catalytically active or not.

1. Introduction. Somorjai's model

For the theoretician who aims at understanding how a metallic surface can induce heterogeneous catalysis, the main difficulty consists in finding a realistic model of the surface. Several models have been widely used.

1) The cluster model [1]: a finite number of metal atoms, those which are locally important, are treated in the calculation, but the "metallic" periodic wave nature of the orbitals is missing. In spite of this drawback much useful information can be obtained.

2) The infinite slab [2]: three or four layers of atoms (with periodic boundary conditions in the two dimensions of the layers) are used to mimic the metal. This model has been successful, under the assumption that the effects of dimensionality perpendicular to the layers dies out rapidly. Because of the periodicity, mostly ideal plain surfaces (of low indices) have been studied.

[1] New address: Laboratoire de Chimie Organique Théorique, URA 506, Bât F, 4 Place Jussieu Université P. et M. Curie. 75252 Paris, France.

[2] Permanent address: Department of Chemistry, Pennsylvania State University. 152 Davey Laboratory, University Park PA16802, U.S.A.

[3] To whom correspondence should be addressed.

3) In rare cases with high symmetry (finite FCC crystals cut along square (100)-type faces) analytical Hückel wave functions exist for the entire metal [3] and can be used to study the approach of simple adsorbates. This model forbids any distortions from ideal surfaces.

Somorjai has suggested to us [4] a model that seeks to compromise between accounting for the periodic nature of the metal (along two of its three dimensions) and also accounting for the exact local nature of the surface, and in particular *its roughness*. He suggests that in a first approximation the rough surface be represented by a single infinite two-dimensional layer–the effect of the underlying layers is assumed to be screened off–on top of which sit, at regular intervals, defects in the form of islands of metal atoms. Each island is surrounded by steps of the type Somorjai himself observed [5]. Such islands might be formed as the surface is created, or when the surface is restructured by the incipient adsorbates [6]. Surface roughening is now well documented by electron diffraction and scanning tunneling microscope studies [7].

In this and the following paper, we have used Somorjai's model to study two successive problems

(1) the effect of island size and shape on the underlattice bond strengths. Here we choose the (100) lattice as an example.

(2) the effect of underlattice symmetry (for fixed island) on the same (following paper).

Each atom is assumed to carry a single s orbital, and the total electron count is allowed to vary from 0 to 2 per atom. Most often, we will speak of a certain percentage (25, 50, 75%) of band filling. In our mind, the variation in band filling (from 0% to 100%, or from 0 electron to 2 electrons per atom) corresponds to sweeping through a transition-metal series in the periodic table. Thus, in a crude manner, 70% corresponds to iron, 80% to cobalt, etc.

The calculations were performed via the extended Hückel method, including periodic boundary conditions. This is known as the "Crystalline Extension of the Extended Hückel Method" or the "Extended Hückel Tight Binding Method" [8]. In such calculations each "block" (a surface of 49 atoms plus the adatoms) *including the island* forms a unit cell which is periodically repeated in two dimensions. After the repeating unit cell is defined, one constructs the Bloch orbitals for the crystal by combining, with the appropriate phase factor, the atomic orbitals equivalent by translational symmetry of all the unit cells. Finally one solves the secular determinant between all the Bloch orbitals (same $\boldsymbol{k}$-values) to generate the crystalline orbitals. The islands are so far from each other that they can safely be assumed to have no influence on one another. Variations with the $\boldsymbol{k}$-vector in the reciprocal space are small.

The metallic s orbital was chosen as a 4s orbital with a Slater exponent 1.74 and a Coulomb energy -12.85 eV. These values fit the FCC band dispersion for the FCC nickel crystal. Overlap integrals at distances larger than 5 Å are neglected. We also carried out preliminary calculations in the following cases:

– simple Hückel restricted to nearest neighbor interactions a) on a 4/49 isolated block (scheme I-SQ but without the periodicity). (The odd number of atoms is a prerequisite of preliminary calculations requiring the island to lie around the symmetry center O), b) on a 4/400 block, but with periodic conditions for the molecular orbitals of the 400 surface atoms.

– Extended Hückel, on the isolated 4/49 block. These calculations will only be referred to briefly in the text. Other calculations, on very small fragments, were also performed to improve the qualitative understanding of the results. Our purpose was to inquire how the islands modify the bond orders (hence the bond strengths) between neighboring surface atoms.

2. A preliminary calculation: the 4/49 case for the FCC(100) surface

Our very first calculation on Somorjai's model was an analytical Hückel-type calculation putting four atoms at the FCC positions on top of a square of 400 atoms. The molecular orbitals in one dimension have well known analytical expressions [7]. In two dimensions, according to their symmetry relative to the Oxz and Oyz planes, they have the form of (cosine or sine) × (cosine or sine) product waves, the four different types of functions corresponding to the four possible symmetries [1] for the 4/400 block: S_xS_y, A_xA_y, S_xA_y and A_xS_y. The secular equations are solved separately for each symmetry type (a common β value [2] of -1 eV is assumed between all neighbors). Typical results are shown in table 1.

The results are remarkable. While all three surface bonds are weakened for small (25%) fillings, the behavior of each bond becomes unique as the filling increases:

– B–C *remains weak* for 50% filling (whereas is the naked surface it strengthens) at 0.3656 versus 0.5205.

– B–D *strengthens so much* that at 75% filling, it surpasses the reference naked surface bond (0.5184 versus 0.4356).

– C–E is relatively unaffected by the island, its bond order remaining close to the naked value.

Our natural reaction was to proceed to a more sophisticated calculation: an extended Hückel calculation on a 4/49 block. The 4 atoms from the island are at the center of the 49-atom square (scheme 1-SQ but without the periodicity). The difference with the previous calculation is that the edges impose a differentiation between the bond orders, even for the reference 49-atom surface. Yet, with the

[1] S_x, A_x, S_y, A_y refer to conservation or inversion of symmetry with respect to the Oxz or Oyz planes.

[2] β is the Hückel resonance integral between φ orbitals on nearest neighbor atoms i and j, $\langle \varphi_i | H | \varphi_j \rangle$.

Table 1
Bond orders for a 4/400 block (Hückel calculation with periodic boundary conditions for surface MOs)

Band filling	Bond	Clean surface without island	Rough surface with island
25%	B–C	0.4356	0.3554
	B–D	0.4356	0.3117
	C–E	0.4356	0.3651
50%	B–C	0.5205	**0.3656**
	B–D	0.5205	0.5150
	C–E	0.5205	0.5229
75%	B–C	0.4356	0.3884
	B–D	0.4356	**0.5184**
	C–E	0.4356	0.4389

island defect and for 50% filling, there is a very significant reversal of bond orders (table 2). For 75% filling, the initial order for the clean surface is maintained, but the difference between B–D and B–C is vastly enhanced in the rough surface. We have also included the D–E bond order, which has a behavior parallel to–but much more weakly–that of B–C.

These results were confirmed in a third preliminary calculation using the simple Hückel method instead of the extended one, revealing the major role of a single MO. For instance, the B–C bond order drops from 0.34 (68e) to 0.25 (70e) while the B–D bond rises from 0.39 to 0.46.

We now turn to the full calculations on the periodic system in which the block of scheme 1-SQ–now treated as a unit cell–is repeated periodically in two dimensions, thus mimicking a "rough" surface with a periodic irregularity (the island is repeated at distant intervals). In such a calculation, the crucial factor is the wave vector $\boldsymbol{k}$ of the reciprocal space which expresses the phase relationship

Table 2
Bond orders (overlap population) for a 4/49 block (EHT aperiodic calculation).

Band filling	Bond	Clean surface without island	Rough surface with island
50% [a]	B–C	0.1514	**0.0713**
	B–D	0.1246	0.1518
	C–E	0.1211	0.1619
	D–E	0.1658	0.1556
75% [b]	B–C	0.0819	0.0108
	B–D	0.1318	**0.2467**
	C–E	0.1549	0.1417
	D–E	0.1002	0.0513

[a] The actual electron counts are 52e and 54e respectively.
[b] The actual electron counts are 68e and 74e respectively.

between the unit cells. To each MO is associated a crystal orbital which is k dependent. In principle, the final results should be integrated over a grid of k-values; this, for instance, is the way to obtain the COOP curves (Crystal Orbital Overlap Populations [10]). However, as the distance between the repeating islands is large, the variation with the k vector is expected to be small. We therefore started by choosing an arbitrary k value (or a set of k values which treats the bonds under investigation in an equivalent manner). For instance, for the 4/49 repeating unit, we choose to average the results for $k = (\pi/2, \pi/2)$ and $k = (\pi/2, -\pi/2)$. In this manner, bond B–D is treated in the same way as bond B–C. The result (fig. 1b) is very close to that from the aperiodic EHT calculation (fig. 1a).

Figure 1c shows the COOP curves for the B–C and B–D bonds in the periodic 4/49 system (integrated over a grid of 16 k points). The curves are qualitatively similar but the COOP curves are smoother. This agreement justifies the correspondence between MOs and COs and therefore will lead us later to interpret the

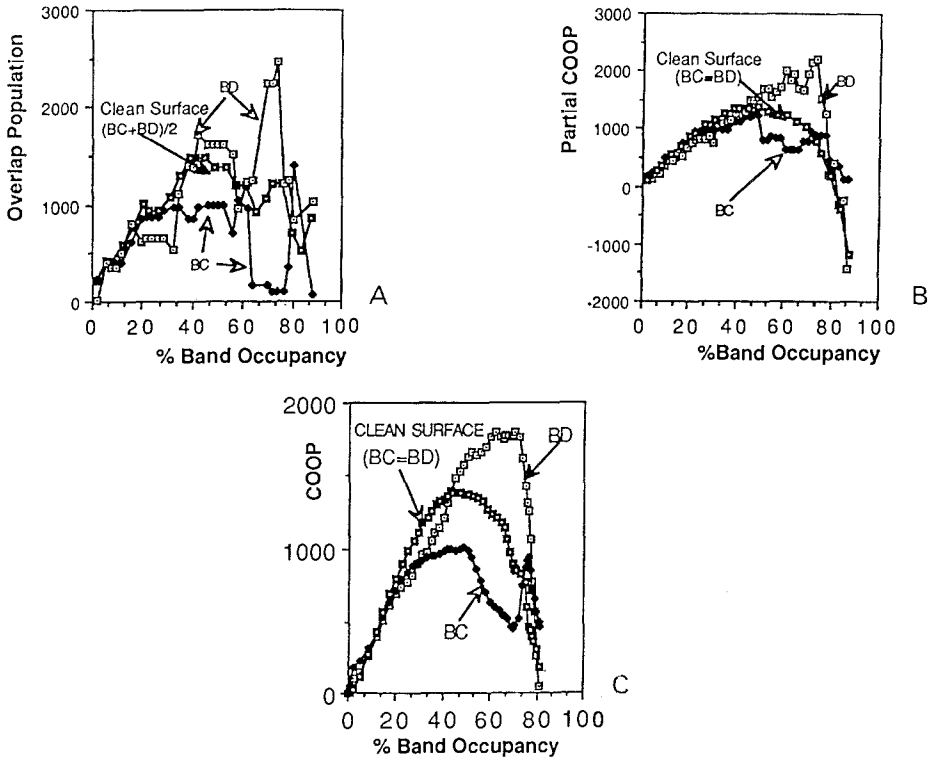

Fig. 1. (a) Overlap population ($\times 10^4$) for the B–C and B–D bonds in the 4/49 system (see scheme 1-SQ) calculated for the aperiodic 4/49 unit (EHT). (b) Integrated Partial Crystal Orbital Overlap population curves (COOP curve)($\times 10^4$) for the B–C and B–D bonds in the 4/49 system (see scheme 1-SQ) calculated for $k = (\pi/2, \pi/2)$ and $k = (\pi/2, -\pi/2)$. (c) Integrated Crystal Orbital Overlap population curves (COOP curve)($\times 10^4$) for the B–C and B–D bonds in the 4/49 system (see scheme 1-SQ) calculated on a grid of k-points of the Brillouin zone.

variations in terms of MOs (see section 4). First of all, the *reference* bond population, for the infinite naked surface, increase, reaches a maximum and then decreases as the orbitals which are (on the average) antibonding become populated. On both curves, the dramatic feature in the weakening of the B–C population, by as much as 50% in the region of half filled band–but recovering at very high occupations–and the concomitant strengthening of the B–D bond for the same electron counts.

3. Other islands: The simple atom, the linear structures and the infinite terrace systems

Encouraged by these results, we have performed a series of calculations for islands of different sizes and shapes on a (100) surface (see scheme 1). The same crystalline extension of the EHT method has been used for the cases illustrated in scheme 1-A(1/49), 1-B(2/49), 1-C(3/49(L)), 1-D(4/49(L)) and 1-E(21/49). The comparison between all the different islands is shown in fig. 2. The differences are dramatic. In fig. 3a and 3b, we run through the entire band occupancy possibilities for both bond B–C and B–D. The behavior for the linear terrace is exactly opposite to that for the square terrace. After an initial rise, the integrated COOP curve remains constant and, thus, passes way below the reference curve for a band filling between 20% and 40%. Then, it suddenly increases and becomes very large in the 40%–60% band filling range. Finally, it strongly decreases at higher fillings.

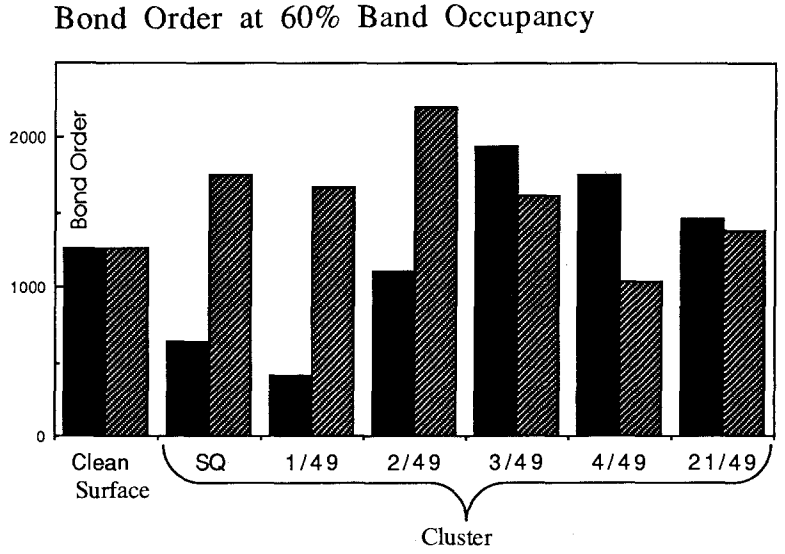

Fig. 2. Overlap Population at 60% band occupancy (bonds B–C and B–D) for clean surface and the different rough surfaces shown in scheme 1.

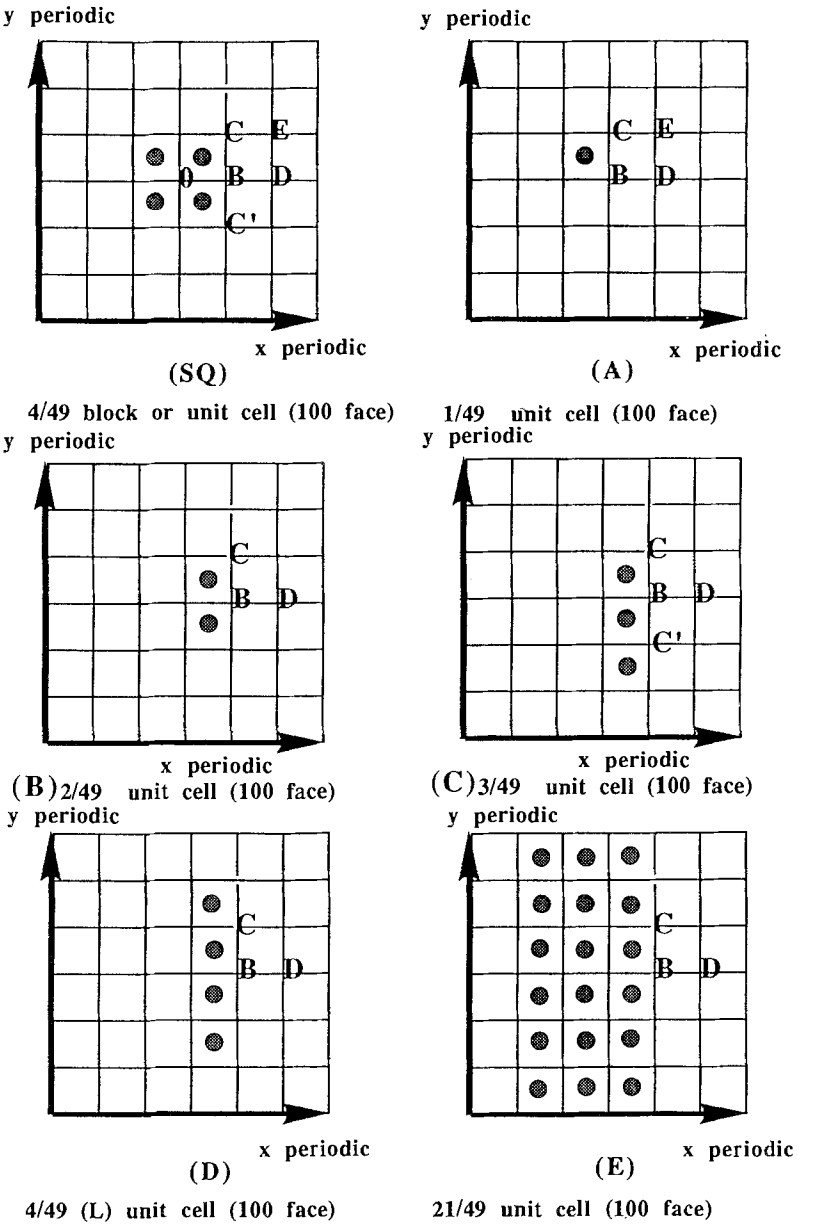

Scheme 1. Different perturbing islands on the 49-atom surface unit cell. Island atoms are shaded.

Naïvely, one might have expected a slight overall intrasurface bond weakening (due to surface-island bonding). Surprisingly some bonds weaken whereas others strengthen, and the observed orientation effects vary from case to case. Clearly, whether a bond such as B–C weakens or strengthens depends

– on the nature of the perturbing island (island specificity)

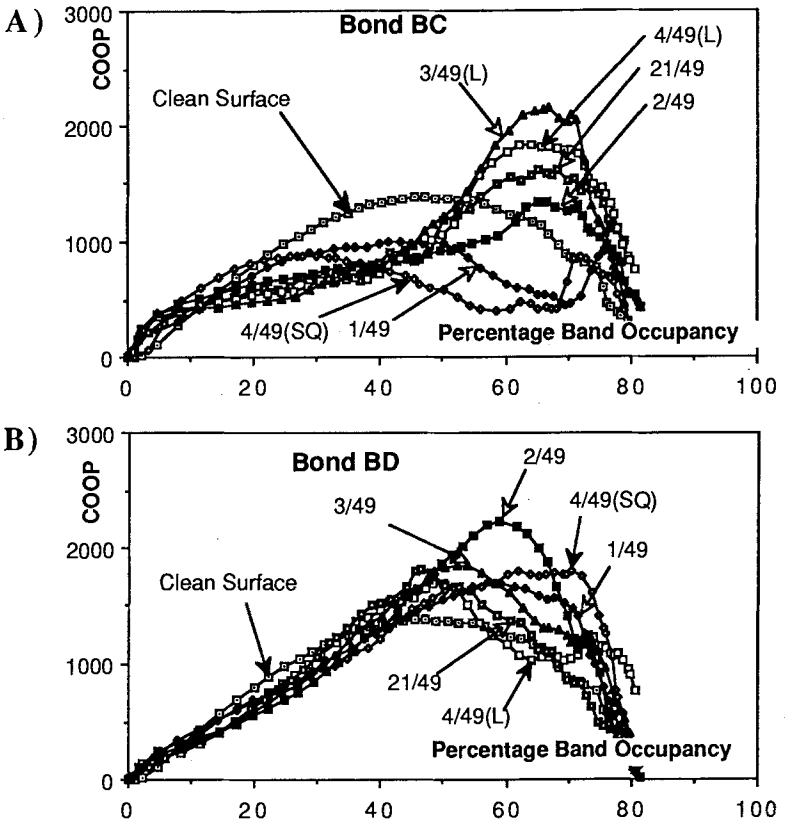

Fig. 3. (a) Integrated COOP curve($\times 10^4$) for the B–C bonds in the various systems (see scheme 1) calculated on a grid of k-points of the Brillouin zone. (b) Integrated COOP curve($\times 10^4$) for the B–D bonds in the various systems (see scheme 1) calculated on a grid of k-points of the Brillouin zone.

– on the band filling (corresponding in a first approximation to a metal specificity).

4. Qualitative interpretation

We attempt to interpret the results from two differing view points.

a) PERTURBING ISLAND BESIDE A LARGE POLYENIC RING

We mimic the 49 unit cell surface (100 face) by the simplest possible periodic chemical system: a cyclic ring of, say, 21 atoms. We calculate its orbitals by the simple Hückel method. The starting MO's must be chosen so as to be symmetric or antisymmetric with respect to the symmetry element introduced by the perturbing island. This leads to two cases.

I) The symmetry plane cuts through the middle of B–C (1/49, 3/49,...). Then the *symmetric* orbitals are B–C-*bonding* and the *antisymmetric* orbitals B–C-*antibonding*. They form two distinct patterns. The partial B–C bond order for the $(j+1)^{\text{th}}$ symmetric orbital

$$\Psi_{j+1} = \frac{2}{\sqrt{21}} \sum_{r=1}^{21} \cos\frac{2\pi j}{21} \text{ is } \frac{4}{21}\cos^2\left(\frac{20\pi j}{21}\right),$$

while the partial bond order for the jth antisymmetric orbitals

$$\Psi'_j = \frac{2}{\sqrt{21}} \sum_{r=1}^{21} \sin\frac{2\pi j}{21} \text{ is } \frac{-4}{21}\sin^2\left(\frac{20\pi j}{21}\right).$$

The net results are shown in figs. 4A and 4B. Integration for the total bond order is shown in fig. 5A (clean surface).

II) The symmetry plane cuts through B (4/49(SQ), 2/49, 4/49(L)...). Then the antisymmetric orbitals can be disregarded (0 amplitude on B, so zero contribution to B–C or B–D strengths). The *symmetric* orbitals turn out to be *both* B–C-bonding and B–C-antibonding. Thus only a single pattern is necessary in this case. The partial bond order is now given by

$$\frac{4}{21}\cos\frac{2\pi j}{21} \text{ for } \Psi_{j+1}$$

as shown in fig. 4C.

The two preliminary decompositions are entirely equivalent for the isolated polyene as can be verified by adding the two patterns A and B of fig. 4, which leads to the pattern C of the same figure. As soon as a perturber is introduced, however, each scheme has its own behavior.

We now turn to the perturbed polyene. We consider successively the 1/49 and 3/49–which belong to case I–the 2/49, 4/49(L)–which belong to case II

Schemes 2a and 2b are supposed to mimic the interaction between P, the island atom and B–C in the 1/49 case and between the 3 island atom and B–C in the 3/49(L) case.

The 1–2 antibonding MO's are unaffected by P so their contribution to the bond order 1–2 is unchanged. The 1–2 bonding orbitals however are mixed together by the perturbation.

– They become either *amplified* or *diminished* by the perturbation.

– They get pushed up and down by P (whose initial energy is nonbonding, $\epsilon = 0$). The end results that those with the *largest* amplitude on 1–2 are either at the very bottom (with the strongest possible bonding interaction with P) or at the very top (with strong antibonding interactions) (fig. 6A). In particular, the lowest symmetric MO gives a combination with P (with large in-phase amplitudes on 1, 2 and P) which drops in energy below the bottom (2β) of the energy band of the ring (see fig. 5A and 6A). It is analogous to the "surface state" of impurities in solids [11].

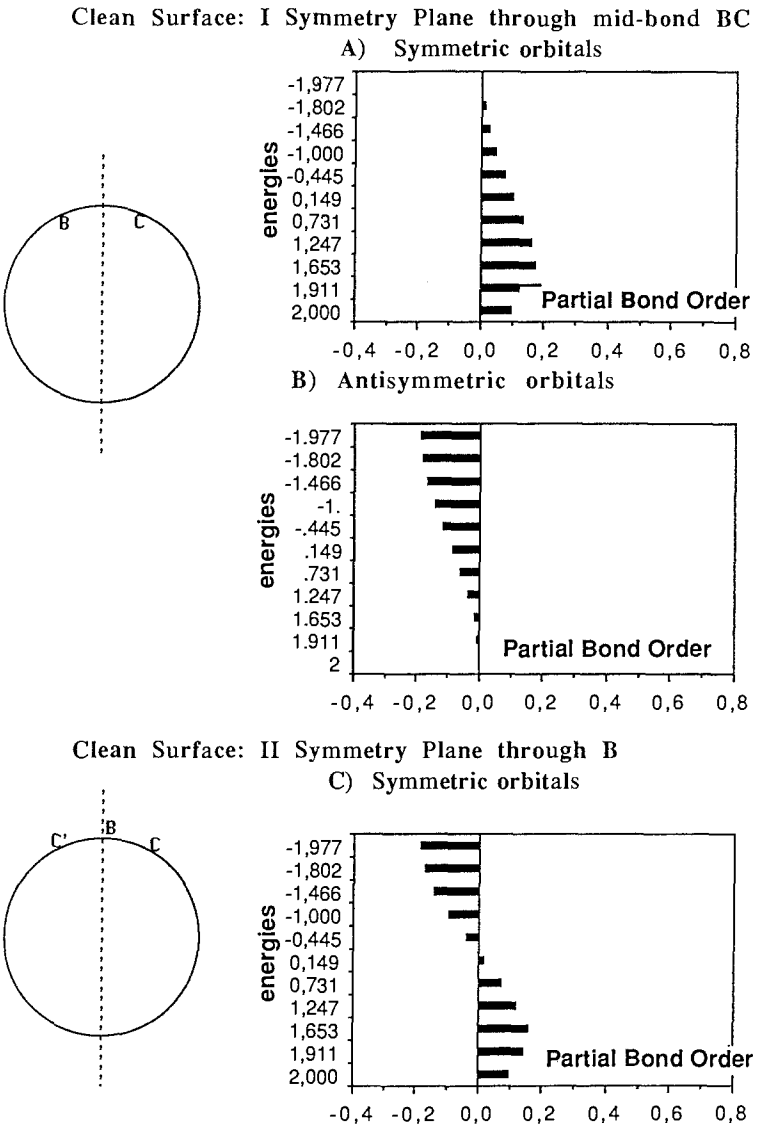

Fig. 4. Partial Bond Order from Hückel calculations for the clean surface modelized as a polyenic ring for the decompositions associated with the symmetry introduced by a perturbing island.

Hence the bond order 1–2 for 2 or 4 electrons in the system starts off higher in the isolated ring (fig. 5A–l.h.s, compare with the far l.h.s. of fig. 3, 1/49 curve). The 1–2 bonding orbitals, after interaction, in the middle energy range have relatively low amplitudes on 1 and 2. Slowly, as the energy (or occupation number) rises, the antibonding orbitals *win out*. As their wave length gets shorter with more and more nodal character in bond 1, 2, the bond order 1–2 decreases, falling sharply below its unperturbed value (fig. 5A).

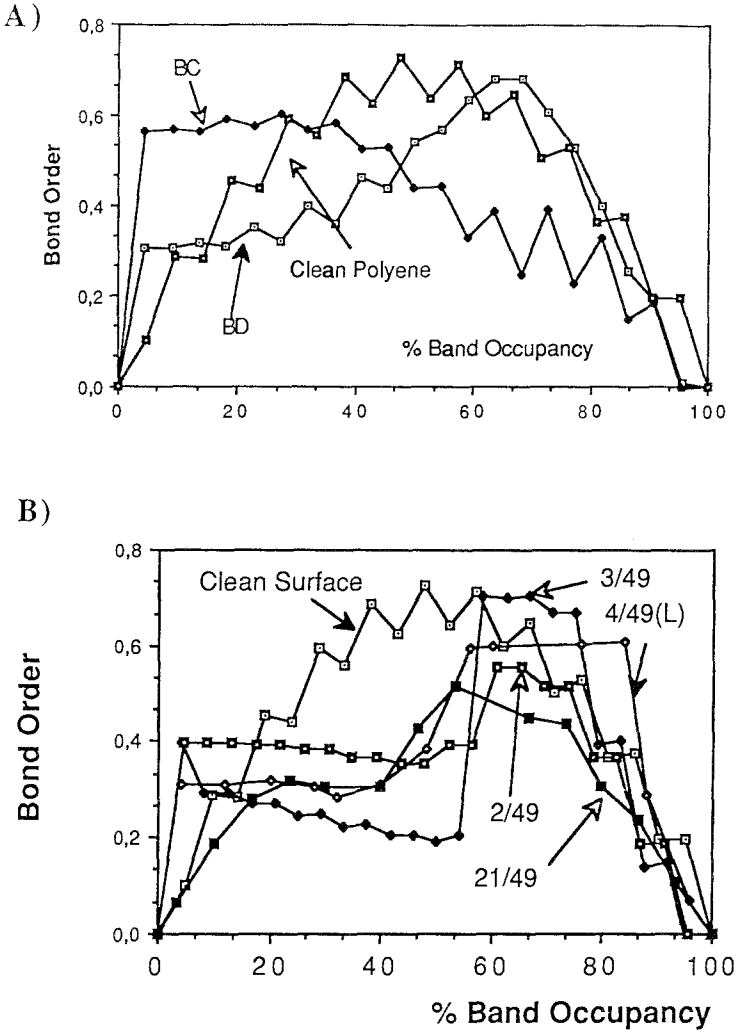

Fig. 5. Bond orders from Hückel calculations (a) scheme 2a (single atom perturber) for bond B–C and B–D versus the electron count; (b) schemes 2b and 2c and 2d versus the band occupancy.

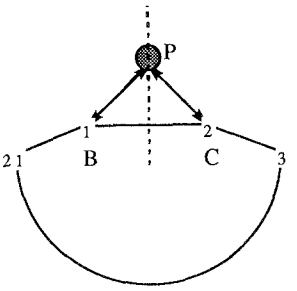

Scheme 2a.

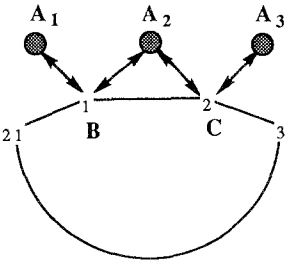

Scheme 2b.

Symmetry Plane through mid-bond BC

A) 1 Atom Perturber Symmetric Orbitals

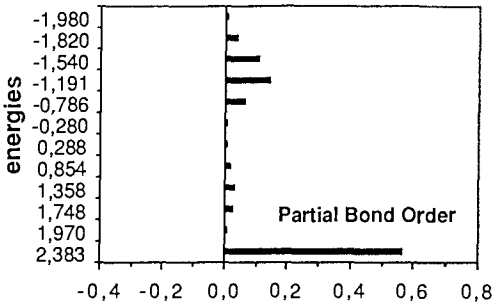

B) 3/49 island - Symmetric Orbitals

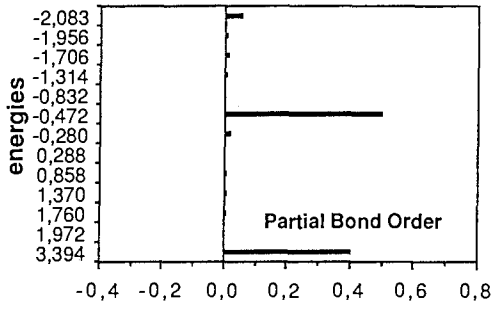

C) 3/49 island - Antisymmetric Orbitals

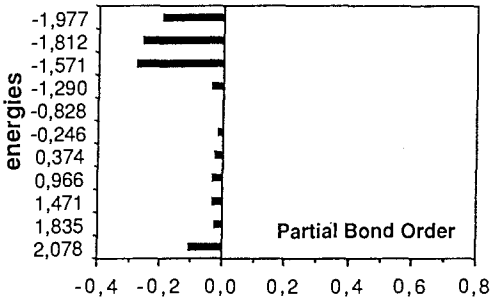

Fig. 6. Partial Bond Order from Hückel calculations for the 1/49 and the 3/49 cases.

It is only at the very top of the energy spectrum where, as we mentioned earlier, the remaining high amplitude 1–2 bonding MO's are gathered, that the bond order stops weakening (fig. 5A) and even increases in the full calculation (fig. 3A, far r.h.s.).

As for bond B–D, the behavior of the bond order 21–1 (or 2–3) in our model perturbed system should have some analogy to its strength. In particular, in the

mid-band region, the 1–2 antibonding MO's have relatively larger concentration than the 1–2 bonding ones (pushed up and down; see above). But for $\epsilon = 0$ the natural wave length of the MO's is four bonds. Their amplitude will often vary as

		C	B	D	
−	+	+	−	−	+
20	21	1	2	3	4

which explains an opposite behavior for B–C and B–D, whence a strengthening of bond B–D from approximately 50% to 70% band occupation (see fig. 5A).

Let now consider directly the 3/49 case, where the atom P is replaced by the atom A_2. Two symmetric orbitals $(^{+}_{A_1}, ^{+}_{A_2}, ^{+}_{A_3})$ and $(^{+}_{A_1}, ^{-}_{A_2}, ^{+}_{A_3})$ interact with the symmetric set. The second one has little effect because of its high energy and small matrix element. The first one, with low energy, interacts fully with the symmetry band precisely where the MO's have their largest amplitude. It creates two large amplitude states: a surface state as before, and a state just above the mid-band at 60% band occupancy (see fig. 6B). Relative to the 1/49 case, these two levels are shifted to lower energies because the perturbing level is itself at lower energies. Also at variance with the 1/49 case, the antisymmetric orbitals also interact with the perturber through its non-bonding $MO(^{+}_{A_1}, ^{0}_{A_2}, ^{-}_{A_3})$. The effects (see fig. 6C) are felt in the middle to upper band region, by a decrease in the amplitude of the middle B–C-antibonding orbitals (whence nearly a void) and an increase in amplitude of the very top B–C-antibonding orbitals. The bond order (fig. 5B) and the COOP values (fig. 3A r.h.s.) strongly increase between 60% and 80% of band filling. The rise results both from the existence of a B–C bonding state and from the absence of practically any antibonding states in that region.

We now consider together the 2/49, 4/49(L) (scheme 2c, 2d) and 4/49(SQ) cases which belong to the second family.

The relevant symmetric polyenic MO's are either B–C-bonding (of type $(^{+}_{C'}, ^{+}_{B}, ^{+}_{C})$ with low energy) or B–C-antibonding (of type $(^{+}_{C'}, ^{-}_{B}, ^{+}_{C})$ with high energy). The interaction with the B–C-bonding states is strong (close energy, large matrix elements) and leads to a low-lying surface state and a few relatively

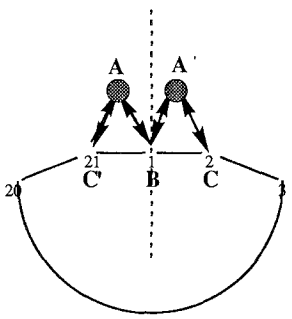

Scheme 2c.

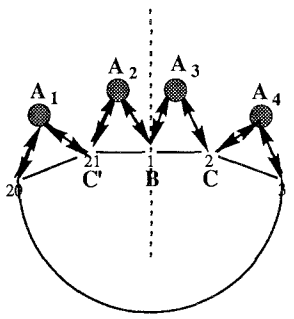

Scheme 2d.

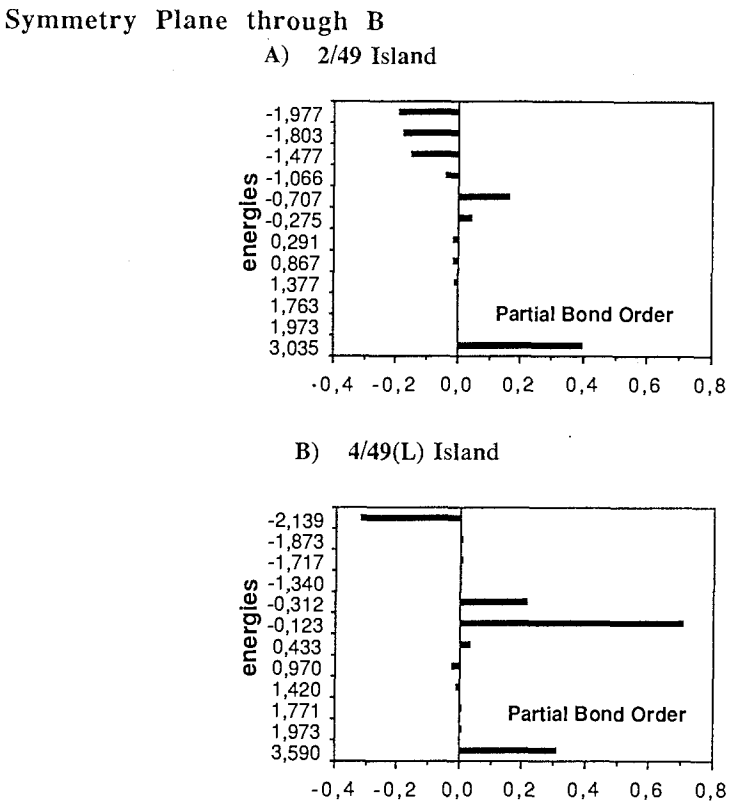

Fig. 7. Partial Bond Order from Hückel calculations for the 2/49 and 4/49 cases. Contributions of the symmetric orbitals.

strongly bonding orbitals at 65% occupation. The B–C-antibonding orbitals, by contrast, interact weakly with the σ^*_{AA} (distant energy, small matrix element); they remain confined to the upper third of the band. The result is that, after a sharp early increase, the B–C bond order *increases again* when the B–C-bonding orbitals (at -0.275β and -0.707β, fig. 7A) are met. For higher occupancies, the decrease in bond order is very similar to that for the clean system (compare 2/49 and the clean surface curves in fig. 3a). Thus the essential difference with the 1/49 case in the *absence* of any B–C-antibonding orbitals at midband to win out. As for the 3/49 case, this absence of B–C-antibonding orbitals is crucial to the rise in bond order.

Now if we go to the 4/49(L) case–scheme 2d–the essential novelty is that the island brings an orbital ($^{+}_{A_1}$, $^{+}_{A_2}$, $^{-}_{A_3}$, $^{+}_{A_4}$) which can interact strongly (particularly because of its high energy, -0.6β) with the B–C antibonding orbitals. Since the island orbital lies below them, it pushes them up to the very top (fig. 7), where they form an antibonding surface state. Thus the B–C-bonding orbitals dominate throughout the entire energy band and the B–C bond order can rise uninhibited, the COOP curve climbing even higher than the reference curve. The effect is

compounded by the fact that the low-lying ($\overset{+}{A}_1$, $\overset{+}{A}_2$, $\overset{+}{A}_3$, $\overset{+}{A}_4$) island orbital pushes the B–C-bonding orbitals upwards so that, relative to the 2/49 case, the lowest surface state has less amplitude and the mid-band orbitals more amplitude (compare figs. 6A and 7B).

Finally a word concerning our model for preliminary calculation, the 4/49(SQ). A Hückel-type calculation of a square island interaction with a 21 polyene in the usual manner leads, not surprisingly, to an orbital pattern close to that of the 2/49–in disagreement with the results of fig. 3 where the net results are parallel to those for 1/49. We feel that the cyclic polyene model is not appropriate here, because all four atoms interact with the surface, something which cannot be mimicked by two atoms bordering a one-dimensional chain. Similarly, we can hardly expect a one-dimensional model to give a realistic account of the 21/49 case.

b) FRAGMENT CALCULATIONS

Now we turn to an entirely different explanation. Let us consider (scheme 1-A) atoms BCDE as an isolated fragment. Let us calculate its Hückel MOs and see how they would be perturbed by an approaching P atom. We will again obtain insight into the weakening of B–C (B–C′) and the concomitant strengthening of B–D. The unperturbed situation can be schematized as below, where the orbitals are classified as **S** or **A** relative to the x symmetry axis.

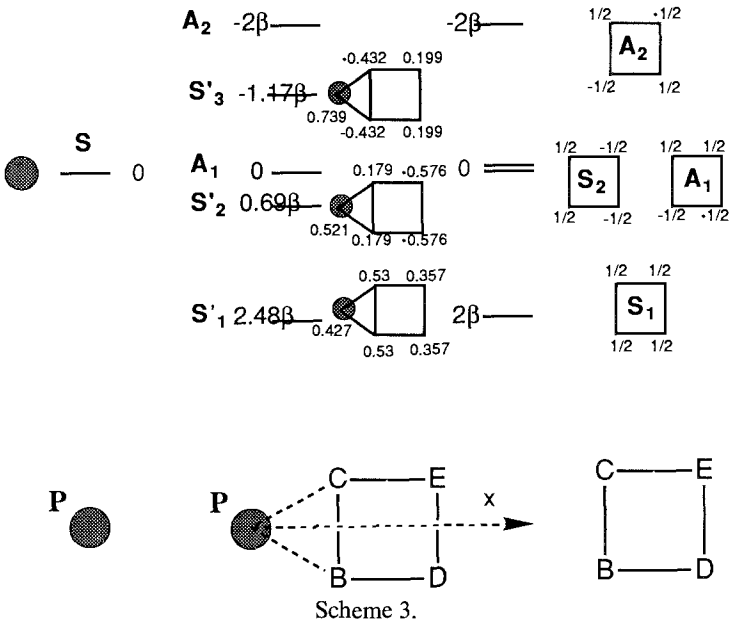

Scheme 3.

Table 3
Bond order for a 5-atom fragment mimicking the 1/49 block (scheme 1-A)

electron count	clean surface	rough surface	
		B–C	B–D
1	0.25	0.281	0.189
2	0.50	0.562	0.379
3	0.50	0.594	0.275
4	0.50	0.626	0.172
5	0.50	**0.376**	**0.422**
6	0.50	**0.126**	**0.672**
7	0.25	0.313	0.586
8	0.0	0.50	0.50
9	–	0.25	0.25
10	–	0.0	0.0

As the two fragments interact, orbital **S** of P mixes with $\mathbf{S}_1$ and $\mathbf{S}_2$, but leaves $\mathbf{A}_1$ and $\mathbf{A}_2$ unchanged. The mixing of the three symmetric orbitals leads to three new symmetric orbitals–one low lying "surface state" $\mathbf{S}_1'$, one weakly bonding orbital $\mathbf{S}_2'$, and one strongly antibonding orbital $\mathbf{S}_3'$ (scheme 3). Only $\mathbf{S}_1'$ and $\mathbf{S}_3'$, at the bottom and the top of the energy range, have large amplitudes on B and C. Thus for the new bond order pattern orbital $\mathbf{A}_1$ dominates the mid band region, as already explained in the interpretation of scheme 2a. Table 3 shows the initial and final bond orders for B–C and B–D. The sharp decrease in B–C bond order and increase in B–D bond order occur as $\mathbf{A}_1$ is filled, i.e. for electron counts of 5 and 6. The fragment calculation even accounts for the initial rise of B–C bond order above the reference value (3 electrons), and its return to a large value at high band filling (8 electrons, 80%).

5. Potential consequences for surface restructuring

The dramatic bond order changes, and bond overlap population changes calculated above imply equally dramatic bond length changes. The relationship between bond order and bond length in conjugated hydrocarbons has been well etablished for more than 30 years (see for instance [12]). The same is true for overlap populations [13]. Furthermore, if sp^2–sp^2 carbon-carbon bond can vary between 1.35 Å (bond order 1) to $\approx$ 1.52 Å (bond order 0), the variations will be even greater in metals. For instance, the Ni–Ni bond in Ni_2 is 2.20 Å [3] [14], while it is 2.49 Å in the metal, and it rises to 2.61 Å and 2.64 Å in the cluster $[Ni_8(CO)_{16}C]^{2-}$, for instance [15]. Thus a drop in overlap population of 50%, or a

[3] The overlap population for Ni_2 two electrons is 0.564. It drops to 0.135 and 0.093 for the (100) and (111) monolayer at 50% band filling.

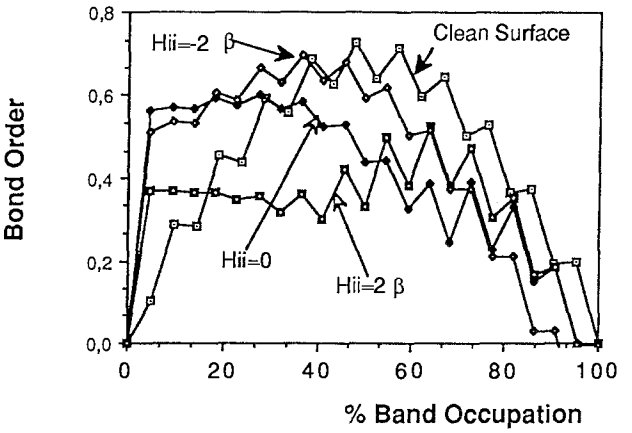

Fig. 8. Bond Orders from Hückel calculations (single atom perturber) for bond B–C for an electronegative island ($H_{ii} = 2\beta$) and for an electropositive island ($H_{ii} = -2\beta$).

rise by nearly 100% as calculated in fig. 2, should imply bond length changes of the order of 0.2 to 0.3 Å.

An immediate consequence of our results is that subsequent surface restructuring will occur. Indeed the *symmetric* underlattice will respond to the *asymmetric* (certain bond shortenings, certain bond weakening) effect induced by the perturbing islands. Although we have not yet allowed the surface atoms to be displaced and form distorted patterns around the islands, clearly our results lend some initial support to the distortions found around atomic adsorbates (carbon on Ni(100) [6c], S on Fe(110) (see in particular ref. [6a], table 2, ref. [6c] and ref. [16]).

We have attempted to study the effect of changing the electronegativity of the islands, in the simplest case of 1/49 (scheme 1-A). In the EHT theory, a change in the Coulomb integral on P implies also a change in the matrix elements between P and the neighboring surface atoms (through a modified Wolfsberg-Helmholtz matrix element). To study the sole effect of Coulomb attraction of P, the single Hückel model of scheme 2a seems more appropriate. The results are shown in fig. 8, for α (Coulomb integral) equal to $\alpha - 2\beta$ and $\alpha + 2\beta$ respectively. For the electropositive atom (first case), the bond order for the "rough polyene" curve resembles that for the "clean" polyene as the level P rises so high as to have little remaining interaction with the significantly B–C-bonding MO's of the polyene. For the electronegative atom ($\alpha + 2\beta$), on the contrary, the level P is very close to the B–C-bonding orbitals of largest amplitude. Hence the surface state is even lower in energy though with more amplitude on P and less on B–C. Furthermore, the group of B–C-bonding orbitals which were pushed up high previously, are pushed up less now and now predominate in the mid-band region, over the B–C-antibonding orbitals which do not yet have very significant amplitude. Thus, for the mid-band occupancy, the bond order rises instead of falling.

6. Potential consequences for heterogeneous catalysis

Our results also show that the island activate the surface for heterogeneous catalysis. Bonds which are weakened by surface roughening–such as bond B–C in case 1A–should be ideal candidates for cleaving incoming adsorbates, such as H_2. Indeed a small bond population means that many atom(B)-atom(C) *antibonding* crystal orbitals are occupied. These orbitals are in the higher energy range since the weakening occurs in the region of 50% to 75% band filling. Hence, from a frontier orbital [17] rationale, these filled *high* lying locally antisymmetric orbitals can interact strongly with the empty locally antisymmetric σ^* orbital of H_2, in a parallel approach:

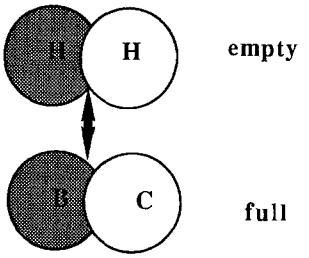

Whether or not the atoms at the termini of the weakened bonds are also good candidates for strong static bonds to the cleaved H atoms–or whether these will have to move elsewhere, thereby providing a mechanism for catalytic turnover–remains totally open to question, since we have not performed any calculations on (island + metal + adsorbate) systems.

Bonds which are strengthened by surface roughening–such as B–D in case 1A would be more like to favor insertion reactions in which an adsorbate comes down on the surface with an empty σ-type orbital pointing at it. Indeed these bonds have a wealth of high lying atom (B)–atom(D) *symmetric* crystal orbitals which can interact nicely, frontier-wise, with the incoming molecule:

Going from case 1(SQ) to cases 1C, for instance, the behavior of bond B–C is reversed. Hence, for a given bond, whether or not catalysis occurs depends on the nature of the island. There is an island specificity.

What is even more striking is that, depending on the number of electrons per atom–which, in our model, corresponds to a variation in the group of transition metal–the same bond may be weakened or strengthened. Hence a *specificity* of the metal concerned is expected. However figs. 2 and 3 show this specificity to be much more significant for large band occupancies than for small ones (hence a possibly much more significant effect in the d^5–d^{10} transition metals). We have not considered the possibility that the H_2 might come down on top of an island or on a step (such as A_1A_2B in scheme 2b).

Although this paper discusses only square lattices, the tendency towards restructuring also occurs for lattices with hexagonal symmetry. The results will be

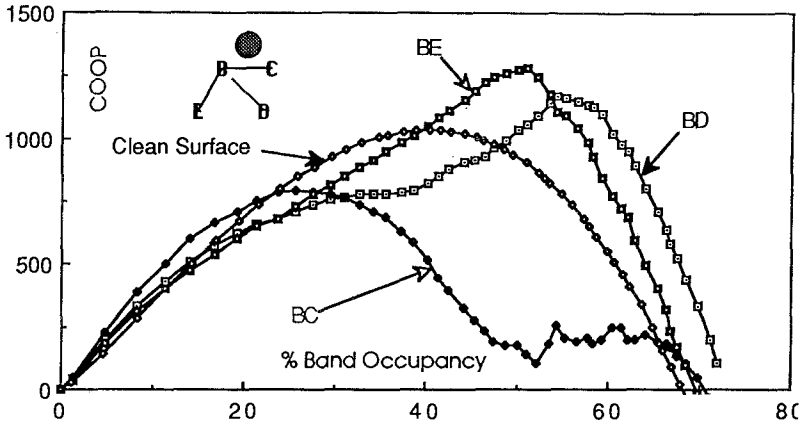

Fig. 9. Integrated COOP curve($\times 10^4$) for bonds B–C and B–D in the 1/49 system of a (111) surface.

dealt with in a separate paper. Here we show simply (fig. 9) the effect of a single island atom on a hollow site of a FCC(111) surface.

Our model has the disadvantages which accompany its great simplicity:

– only a single s orbital is located on each atom; the next step will be to see whether the effects survive in a (5d, 1s, 3p) 9-orbital model.

– only a single layer of atoms has been used to model the clean surface; the next step will be to account in a more sophisticated manner for the surface roughness. In particular, bond strengthening and bond weakening might be enhanced by adequate positioning of *close* superficial islands. For instance the situation:

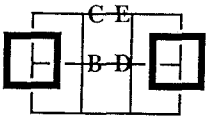

Scheme 4.

should lead to even stronger BD bonds and even weaker B–C ($\equiv$ D–E) bonds. Indeed we saw (table 2) that in case 1-SQ bond D–E mimics the behavior of B–C, so that on each bond (B–C or D–E) the island effects reinforce (as they do also on B–D, in the opposite direction).

– the number of surface atoms in repeating unit cell has been limited to 49. However comparison of the B–C bond order curves for the 1/49 (scheme 1) and a 1/64 system shows an extremely similar behavior (fig. 10).

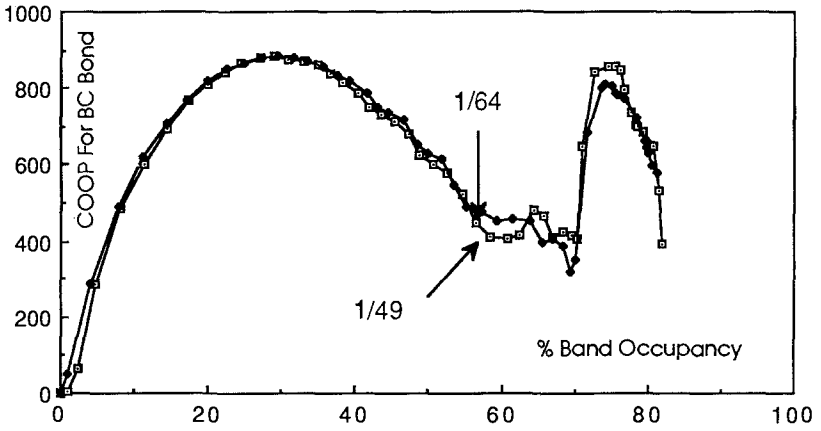

Fig. 10. Integrated COOP curve($\times 10^4$) for bond B–C in the 1/49 and 1/64 systems of a (100) surface.

Acknowledgements

The authors would like to thank Enric Canadell for many stimulating discussions and for helpful advice and Michel VanHove for his comments on the manuscript. They are grateful to him, to Claude Leforestier, Michel Pélissier, Frédéric Lequéré and to Jean-Frédéric Riehl for their help in implementing some of the programs. Last but not least, they thank Gabor Somorjai for his fruitful suggestion and for many helpful discussions.

References

[1] J.N. Allison and W.A. Goddard III, Surf. Sci. 115 (1982) 553;
A. Rosen, E.J. Baerends and D.E. Ellis, Surf. Sci. 82 (1979) 139;
P.S. Bagus, Phys. Rev. B 23 (1981) 2065; Phys. Rev. B 23 (1981) 5464;
A. Gavezzotti and M. Simonetta, Surf. Sci. 99 (1980) 453;
A.B. Anderson and T. Hubbard, Surf. Sci. 99 (1980) 384.

[2] a) C. Thuault-Cytermann, M-C. Desjonquères and D. Spanjaard, J. Phys. C. Solid. State Phys 16 (1983) 5689;
J. Jardin, M-C. Desjonquères and D. Spanjaard, Surf. Sci. 162 (1985) 224.
b) J.-Y. Saillard and R. Hoffmann, J. Amer. Chem. Soc. 106 (1984) 2006.

[3] L. Salem, J. Phys. Chem. 89 (1985) 5576.

[4] G.A. Somorjai, private communication (Jan 31, 1989).

[5] G.A. Somorjai, in: *Chemistry in Two Dimensions: Surfaces* (Cornell University Press, Ithaca 1981).

[6] a) G.A. Somorjai and M.A. Van Hove, Progr. Surf. Sc. 30 (1989) 201;
b) R.M. Nix and G.A. Somorjai, Perspectives in quantum chemistry (Plenary Lectures of the 6th Int. Congress in Quantum Chemistry, 1988) eds. J. Jortner and B. Pullman (Kluwer Academic Publishers, Dordrecht, 1989) p. 97;
c) J.F. Onuferko, D.P. Woodruff and B.W. Holland, Surf. Sci. 87 (1979) 357.

[7] B. Marchon, D.F. Ogletree, M. Salmeron and W. Siekhaus, J. Vac. Sci. Technol. A6 (1988) 531; G.A. Somorjai and M.A. Van Hove, Cat. Lett. (1988) 433;
M.A. Van Hove, R.J. Koestner, P.C. Stair, J-P. Bibérian, L.L. Kesmodel, I. Bartos and G.A. Somorjai, Surf. Sci. 103 (1981) 189;
M. Henzler, Surf. Sci. 19 (1970) 159;
R.W. Joyner and G.A. Somorjai, in: *Surface and Defect Properties of Surfaces*, eds. M.W. Roberts and J.M. Thomas, Vol 2 (The Chem. Soc. Publ. London, 1973) p. 1.

[8] a) M.-H. Whangbo and R. Hoffmann, J. Amer. Chem. Soc. 100 (1978) 6093;
b) C. Minot, M.a. Van Hove and G.A. Somorjai, Surf. Sci. 127 (1982) 441.

[9] L. Salem, *The Molecular Orbital Theory of Conjugated Systems* (Benjamin, N.Y., 1966) p. 117, and equations (3–30) for the case of 6 atoms.

[10] R. Hoffmann and C. Zheng, in: *Quantum Chemistry-The Challenge of Transition Metals and Coordination Chemistry*, ed. A. Veillard (D. Reidel Publishers, 1986) p. 425;
J. Silvestre and R. Hoffmann, Langmuir 1 (1985) 621.

[11] a) F. Seitz, *The Modern Theory of Solids* (McGraw-Hill, New York , 1940) p. 325;
b) J. Friedel, Advances Physics 45 (1954) 446, in particular sections 2.1.1;
c) S. Golden, J. Koutecky and L. Salem studies some years ago the surface states formed by attaching two atoms at the end of a linear polyenic chain (abstract submitted to the 6th ICC Congress, London, 1976, unpublished).

[12] L. Salem, *The Molecular Orbital Theory of Conjugated Systems* (Benjamin, N.Y., 1966) p. 134.

[13] R.S. Mulliken, J. Chem. Phys. 23 (1955) 1833, 1841, 2338, 2343; 26 (1962) 3428;
F. Pilar, *Elementary Quantum Chemistry* (McGraw-Hill, N.Y., 1968) p. 499.

[14] For a review article see: M.D. Morse, Chem. Rev. 86 (1986) 1049. From high resolution studies of optical bands: M.D. Morse, G.P. Hansen, P.R.R. Langridge-Smith, L.-S. Zheng, M.E. Geusic, D.L. Michalopolous and R.e. Smalley, J. Chem. Phys. 80 (1984) 5400. Theoretical calculations give 2.21 Å (EHT-A.B. Anderson, J. Chem. Phys. 66 (1977) 5108), 2.18 Å (local spin densities- J. Harris and R.O. Jones, J. Chem. Phys. 70 (1979) 830) and 2.28 Å (RHF-A. Wolf and H.-H. Schmidtke, Int. J. Quantum Chemistry 40 (1980) 239.

[15] Inorg. Chem. 24 (1985) 117.

[16] W. Pushta, W. Nitchtl, W. Oed, N. Bickel, K. Heinz and K. Mueller, to be published;
W. Oed, B. Doetsch, L. Hammer, K. Heinz and K. Mueller, to be published.

[17] K. Fukui, Topics in Current Chemistry 15 (1970) 1.